Residues 293 and 294 Are Ligand Contact Points of the Human Angiotensin Type 1 Receptor †

ARTICLE *in* BIOCHEMISTRY · JANUARY 2003

Impact Factor: 3.02 · DOI: 10.1021/bi0258602 · Source: PubMed

Residues 293 and 294 Are Ligand Contact Points of the Human Angiotensin Type 1 Receptor†

Jacqueline Pérodin,‡ Maud Deraët,‡ Mannix Auger-Messier, Antony A. Boucard, Lenka Rihakova, Marie-Ève Beaulieu, Pierre Lavigne, Jean-Luc Parent, Gaétan Guillemette, Richard Leduc, and Emanuel Escher*

Département de pharmacologie, Faculté de médecine, Université de Sherbrooke, 3001 12e Avenue Nord, Sherbrooke, Québec, J1H 5N4, Canada

Received March 25, 2002; Revised Manuscript Received October 4, 2002

ABSTRACT: The human angiotensin II type 1 receptor (hAT_1) was photolabeled with a high-affinity radiolabeled photoreactive analogue of AngII, ^{125}I-[Sar^1, Val^5, *p*-Benzoyl-L-phenylalanine^8]AngII (^{125}I-[Sar^1,Bpa^8]AngII). Chemical cleavage with CNBr produced a 7 kDa fragment (285−334) of the C-terminal portion of the hAT_1. Manual Edman radiosequencing of photolabeled, per-acetylated, and CNBr-fragmented receptor showed that ligand incorporation occurred through Phe^{293} and Asn^{294} within the seventh transmembrane domain of the hAT_1. Receptor mutants with Met introduced at the presumed contact residues, F293M and N294M, were photolabeled and then digested with CNBr. SDS−PAGE analysis of those digested mutant receptors confirmed the contact positions 293 and 294 through ligand release induced by CNBr digestion. Additional receptor mutants with Met residues introduced into the N- and C-terminal proximity of those residues 293 and 294 of the hAT_1 produced, upon photolabeling and CNBr digestion, fragmentation patterns compatible only with the above contact residues. These data indicate that the C-terminal residue of AngII interacts with residues 293 and 294 of the seventh transmembrane domain of the human AT_1 receptor. Taking into account a second receptor−ligand contact at the second extracellular loop and residue 3 of AngII (Boucard, A. A., Wilkes, B. C., Laporte, S. A., Escher, E., Guillemette, G., and Leduc, R. (2000) *Biochemistry 39*, 9662−70) the Ang II molecule must adopt an extended structure in the AngII binding pocket.

The octapeptide hormone AngII is implicated in the regulation of multiple cardiovascular functions, such as blood pressure and electrolyte homeostasis (*1*). AngII recognizes with high affinity two distinct mammalian receptor types, AT_1 and AT_2. To date, practically all known physiological functions of AngII have been attributed to its interaction via the AT_1 receptor. As for AT_2, recent studies have suggested that it could serve as a physiological antagonist of AT_1-mediated pressor response, that it could regulate central nervous system functions including behavior, and that it exerts growth inhibitory as well as proapoptotic effects (*2*−*4*). Both AT_1 and AT_2 have been cloned and are members of the vast family of G-protein coupled receptors (GPCRs) (*5*−*8*) but their similarity at the amino acid level is quite low (34%).

Elucidating the stereochemistry of the ligand−receptor interaction is paramount to the understanding of the mechanism by which GPCRs are activated. Site-directed mutagenesis and chimeric receptors are very useful approaches to identify the amino acids involved in ligand binding. Unfortunately, these rather indirect methods could also change the finer architecture of the receptor by affecting intrinsic protein interactions, thus not necessarily reflecting the natural behavior of the ligand in its binding pocket. Site-directed mutagenesis is still the most frequently used tool for studies on peptidergic GPCR's, among them AT_1. Generally, it was inferred that peptidic ligand interaction should occur at the outer surface of their cognate receptors. Combined with conformational studies of the free peptide ligands in various solvents, a more or less folded bioactive structure was proposed, compatible only with a putative binding domain in the extracellular portion or at the interface of the cell surface (*9*−*11*). This situation is quite typical for AngII but also for other bioactive peptides. Consequently, several groups have developed more direct approaches to map the ligand-binding pockets. One of these consists of

† J.P. is a recipient of a studentship from the Heart and Stroke Foundation of Canada (HSFC). This work is part of the thesis of J.P. and M.D. M. A.-M. is a recipient of a studentship from the Conseil de Recherche en Sciences Naturelles et en Génie du Canada. A.A.B. is a recipient of a studentship from the Fonds formation chercheurs & aide recherche. L.R. is a recipient of a scholarship from the Ministry of Education of the Province of Quebec. J.-L.P. is recipient of a CIHR New Investigator Award and R.L. is Scholar of the Fonds de la Recherche en Santé du Québec. E.E. is recipient of a J. C. Edwards chair in cardiovascular research. This work was supported by grants MT13193 and MT7242 from the Medical Research Council of Canada to R.L., G.G., and E.E., as well as from the Quebec chapter of the HSFC to E.E.

* To whom correspondence should be addressed. Tel: (819) 564-5346. Fax: (819) 564-5400. E-mail: e.escher@courrier.usherb.ca.

‡ Both authors contributed equally to the present study.

[1] Abbreviations: AngII, angiotensin II; AT_1 and AT_2, angiotensin type 1 and type 2 receptors; Bpa, *p*-Benzoyl-L-phenylalanine; CNBr, cyanogen bromide; DMEM, Dubelcco's modified Eagle's medium; Endo Lys-C, endoproteinase Lys-C; FBS, fetal bovine serum; GPCR, G-protein coupled receptors; IP_2, inositol bisphosphates; IP_3, inositol trisphosphates; PBS, phosphate buffered saline; PCA, perchloric acid; PITC, phenylisothiocyanate; PVDF, polyvinylidene fluoride; sulfo-NHS-acetate, sulfosuccinimidyl acetate; TFA, trifluoroacetic acid.

10.1021/bi0258602 CCC: $22.00
Published on Web 11/05/2002

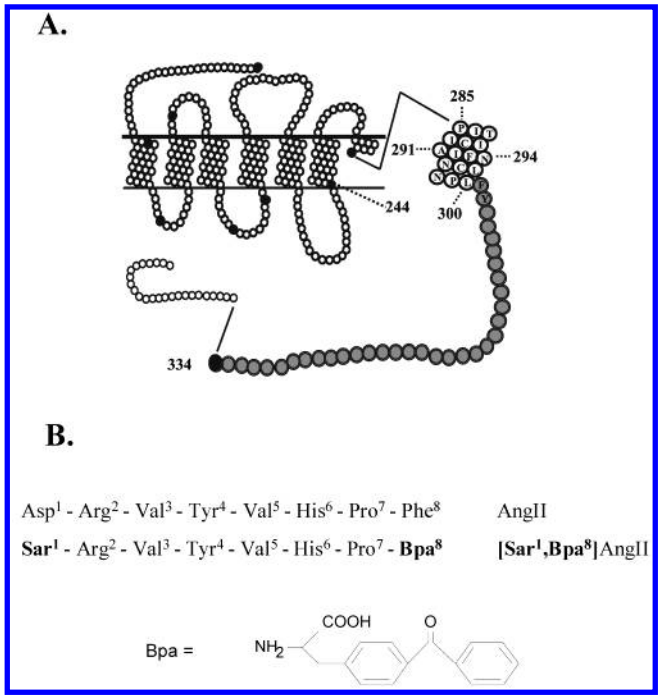

FIGURE 1: Schematic sequence of the hAT$_1$ receptor and of the labeling peptide. (A) The residues of the C-terminal fragment starting with Pro^{285} are large circles, the target sequence Pro^{285}-Leu^{300} are open circles. All Met residues in the sequence are indicated as black dots. (B) Primary structures of AngII, of [Sar^1,-Bpa^8]AngII and of L-*p*-benzoylphenylalanine (Bpa).

labeling the receptor with a photoactive ligand before limited proteolysis and/or chemical cleavage of the covalent ligand/receptor complex. The identification of ligand-binding domains with this technology has been performed on the AngII receptors (*12*, *13*) but also on several other receptors, including the cholecystokinin receptor (*14*), the vasopressin receptor (*15*), the nicotinic acetylcholine receptor (*16*), the substance P receptor (*17*), and the secretin receptor (*18*). Our earlier results with photolabeled hAT$_1$ receptor and limited proteolysis (*12*) seemed to differ from the generally accepted view of peptide ligand binding since the contact of the C-terminal amino acid must occur on a short portion of the seventh transmembrane segment limited by residues 285 and 295, the central segment of the transmembrane domain of hAT$_1$ (Figure 1B). An exhaustive retrospective analysis of most AT$_1$ mutagenesis studies has been published recently (*19*). Its conclusions are ruling out all previous receptor models except our previous model of ligand interaction (*20*). Furthermore, a bent peptide conformation in the biologically active, i.e., receptor bound form, was assumed from physicochemical studies of the AngII molecule (*21*, *22*). Recent results on cyclized AngII analogues show, however, that biological activity is associated to an extended peptide conformation and not to a bend in the peptide's central portion (*23*).

To support this rather unorthodox view of a receptor peptide ligand bound in an extended form and in order to assess the precise location of the C-terminal part of the AngII molecule in the AT$_1$ receptor, we intended to determine the exact contact sites between the C-terminal end of AngII and the hAT$_1$ receptor using an AngII analogue containing a photoreactive moiety in position 8, [Sarcosine^1, Val^5, *p*-Benzoyl-L-phenylalanine^8]AngII ([Sar^1,Bpa^8]AngII, Figure 1B). The hAT$_1$ receptor, transiently expressed in COS-7 cells, was photolabeled and then submitted to chemical cleavage before sequential degradation by the Edman reaction. With this approach, we now show that position 8 of the photolabel is in close proximity of Phe^{293} and Asn^{294} in the seventh transmembrane domain of the hAT$_1$ receptor. This result was then confirmed with hAT$_1$ receptor mutants where Phe^{293}, Asn^{294}, and other residues in this area were successively substituted with Met, photolabeled and subjected to CNBr cleavage. Ligand release confirmed the correct assignment of the two contact points, showing that Phe^{293} and Asn^{294} are in contact with the C-terminal residue of AngII.

The purpose of the present paper is 2-fold: First, we would like to propose new approaches to identify exact contact points in target proteins by a ligand-release strategy, and second, to evidence this transmembrane orientation of a peptide ligand in its cognate receptor and its consequence on receptor activation mechanisms.

EXPERIMENTAL PROCEDURES

Materials. BSA and CNBr were from Sigma (Oakville, ON). PITC and sulfo-NHS-acetate were from Pierce (Rockford, IL). Immobilon-P^{SQ} PVDF membranes were from Millipore (Bedford, MA). Endo Lys-C (EC 3.4.21.50) was from Boehringer Mannheim (Laval, QC). Dr. S. Meloche (Université de Montréal) kindly provided the cDNA clone of the hAT$_1$ receptor. Lipofectamine and culture media were obtained from Gibco BRL (Gaithersburg, MD). [Sar^1,Bpa^8]-AngII was synthesized in our laboratory by the solid phase method and purified by high performance liquid chromatography (HPLC) as previously described (*24*). ^{125}I-AngII and ^{125}I-[Sar^1,Bpa^8]AngII (1000 Ci/mmol) were prepared with Iodogen (Pierce, Rockford, IL) as described by Fraker and Speck (*25*) but in an acetic acid buffer (pH 5.4). The radiolabeled peptides were purified by HPLC on a C-18 column (Waters, Mississauga, ON) with a 20−40% acetonitrile gradient in 0.2% aqueous trifluoroacetic acid (TFA). The specific radioactivity of the radiolabeled peptides was determined by self-displacement and saturation binding analysis.

Site-Directed and PCR Mutagenesis. Site-directed mutagenesis was performed as previously described (*26*) for the mutants F293M-, N294M-, and A291N-hAT$_1$. Briefly, the codon changes in the hAT$_1$ receptor cDNA were made using an in vitro mutagenesis kit (Sculptor, Amersham) based on the phosphorothioate technique (*27*). The mutagenic primers are as follows (altered nucleotides are underlined): Phe^{293}→Met^{293}(F293M-hAT$_1$), 5′-CAGGCAATTGTTCATAT-AAGCTATACA-3′; Asn^{294}→Met^{294} (N294M-hAT$_1$), 5′-GATTCAGGCAATTCATAAAATAAGCTAT-3′; Ala^{291}→M^{291} (A291M-hAT$_1$), 5′-GCAATTGTTAAAATACATTATA-CAAATGGT-3′.

Once the mutation confirmed by DNA sequencing, the cDNAs were excised from M13mp19RF by digestion with *Hind*III and *Xba*I and subcloned into the multiple-cloning site of pcDNA3 previously digested by the same restriction enzymes.

For the second series of hAT$_1$ mutants, codon changes were made with the PCR (Expand High Fidelity PCR system from Roche Diagnostics). PCR mutagenesis experiments were performed, as described by the manufacturer, using the

following oligonucleotides: L300M-hAT$_1$ forward (5′-TGC CTG AAT CCT ATG TTT TAT GGC TTT CTG-3′), L300M-hAT$_1$ reverse (5′-CAG AAA GCC ATA AAA CAT AGG ATT CAG GC-3′), M284L,I290M-hAT$_1$ (5′-TGTA-GAATTGCAGATATCGTGGACACGGCCCTGCCTATC-ACCATTTGTATGGCTTATTTTAAC-3′), M284L,N294M--hAT$_1$ (5′-TGTAGAATTGCAGATATCGTGGACACGGC-CCTGCCTATCACCATTTGTATAGCTTATTTTATGAA-TTGCCTGAATC-3′), M284L,L300M-hAT$_1$ (5′-TGTAGA-ATTGCAGATATCGTGGACACGGCCCTGCCTATCACCAT-TTGTATAGCTTATTTTAACAATTGCCTGAATCCTATGT-TTTATGGCTTTC-3′), as well as the external primers T7 (5′-TAA TAC GAC TCA CTA TAG G-3′) and SP6 (5′-GAC ACT ATA GAA TAG AAT AGG GCC CTC TAG A-3′).

Subcloning into hAT$_1$-pcDNA3 was facilitated by the introduction of a silent mutation in position 279 of the amino acid sequence of hAT$_1$, thus producing an EcoRV restriction site.

Cell Culture and Transfection of COS-7 Cells. COS-7 cells were grown in DMEM supplemented with 2 mM L-glutamine, 100 IU/ml penicillin, 100 μg/mL streptomycin, and 10% [v/v] FBS. Cells were seeded in 10 cm^2 plates and, at ~80% of confluence, were transiently transfected with 4 μg of plasmid DNA and 25 μL of Lipofectamine in 8 mL of serum-free DMEM. The cells were incubated for 5 h at 37 °C and the media were replaced with complete DMEM containing 100 IU/mL of penicillin and 100 μg/mL of streptomycin. 48 h after the initiation of transfection, the cells were washed once with PBS (137 mM NaCl, 0.9 mM $MgCl_2$, 3.5 mM KCl, 0.9 mM $CaCl_2$, 8.7 mM Na_2HPO_4, and 3.5 mM $NaHPO_4$) and immediately stored at −80 °C until needed.

Saturation Studies and Photoaffinity Labeling. Transfected COS-7 cells were subjected to a freeze/thaw cycle for 1−2 min and warmed to 37 °C. The broken cells were then gently scraped, resuspended in 10 mL of binding buffer without BSA (25 mM Tris-HCl (pH 7.4), 100 mM NaCl, and 5 mM $MgCl_2$) and centrifuged for 10 min at 4 °C and 500*g*. The pellet was dispersed in a binding buffer containing 0.1% [w/v] BSA. For saturation studies, the broken cell suspension (50−80 μg of proteins) was incubated for 60 min at room temperature in the presence of increasing concentrations of ^{125}I-AngII (100 Ci/mmol). Nonspecific binding was measured in the presence of 1 μM of unlabeled AngII. Bound radioactivity was separated from free ligand by filtration through GF/C filters presoaked in binding buffer containing BSA. Binding affinities (K_D) and receptor expression levels (Bmax) were calculated by saturation analysis. For photolabeling studies, the broken cell suspension (1 mg of protein) was incubated for 90 min at room temperature in the presence of 3 nM of ^{125}I-[Sar^1,Bpa^8]AngII. After centrifugation at 500*g*, the broken cells were washed once and resuspended in 0.8 mL of ice-cold binding buffer (without BSA), then irradiated for 60 min on ice under filtered (Raymaster black light filters No 5873, Gates and Co. Inc., Franklin Square, NY) UV light (365 nm) (100 W mercury vapor lamp serial no. JC-Par-38, Westinghouse, Pittsburgh, PA). After centrifugation for 10 min at 4 °C and 2500*g*, the pellet was solubilized for 30 min at 4 °C in RIPA buffer (50 mM Tris/HCl (pH 8), 150 mM NaCl, 0.5% [w/v] deoxycholate, 0.1% [w/v] SDS, and 1% [v/v] Nonidet P-40). The cell lysate was centrifuged for 15 min at 4 °C and 15000*g* to remove insoluble material, and the supernatant was kept at −20 °C until needed.

Inositol Phosphate Production. Some 24 h post-transfection, COS-7 cells were labeled with 15 μCi/ml *myo*-[^{3}H]-inositol in inositol-free DMEM medium. After an 18 h labeling period, the cells were washed once with PBS containing 0.1% [w/v] dextrose and preincubated for 30 min at 37 °C in Medium 199 containing 10 mM LiCl, 0.1% BSA [w/v], pH 7.4, 25mM Hepes. Cells were stimulated with 100 nM AngII for 20 min in the same medium. Incubation was stopped by the addition of PCA (5% [v/v]). Cells were scraped and centrifuged for 15 min at 4 °C and 15000*g*. Inositol phosphates were then extracted from the supernatant with an equal volume of a mixture of 1,1,2-trichlorotrifluoroethane and tri-*n*-octylamine (1:1). The samples were vigorously mixed and centrifuged for 1 min at 15000*g*. The upper phase (aqueous), containing the inositol phosphates, was applied to an AG1-X8 resin column. [^{3}H]inositol-labeled compounds were sequentially eluted by addition of ammonium formate/formic acid mixtures of increasing ionic strength, as described (*28*). Inositol bisphosphates (IP_2) and inositol trisphosphates (IP_3) were summed in order to evaluate the phospholipase C activity.

Partial Purification of the Labeled Complex. The photolabeled solubilized receptors were diluted in an equal volume of 2× Laemmli buffer (120 mM Tris-HCl (pH 6.8), 20% [v/v] glycerol, 4% [w/v] SDS, 200 mM DTT, and 0.05% [w/v] bromophenol blue) and incubated for 60 min at 37 °C. SDS−PAGE was done as described (*29*) using a 1.5 mm 7.5% polyacrylamide preparative gel. The gel was then cut into slices and their radioactive content was measured by a γ-counter. The labeled receptor was passively eluted from the gel slices into fresh electrophoresis buffer (25 mM Trizma Base (pH 8.3), 250 mM glycine, and 0.1% [w/v] SDS) for 3−4 days at 4 °C with gentle agitation as described by Blanton and Cohen (*30*). The eluate (~40 mL) was concentrated to a final volume of 0.5 mL using Centriprep-10 and Centricon-10 (Amicon, Berverly, MA) and was stored at −20 °C.

Digestion with CNBr. For CNBr hydrolysis, the partially purified photolabeled receptor (20,000−100,000 cpm) was resuspended in 200 μL of 50% [v/v] TFA before adding CNBr (200 μL) to obtain a final concentration of 100 mg/mL. The samples were incubated at room temperature, in the dark, for 16−18 h. The reaction was terminated by adding 3 mL of water. Samples were lyophilised and resuspended in Laemmli buffer to be analyzed by 16.5% SDS−PAGE Tris-Tricine gels (BioRad, Mississauga, ON) followed by autoradiography on X-ray films (Kodak BIOMAX MS, Rochester, NY). ^{14}C-labeled low molecular protein standards (Gibco BRL, Gaithersburg, MD) were used to determine the apparent molecular weights M_r. Running conditions and fixation of gels were done according to the manufacturer's protocol.

Edman Degradation (Radiosequencing). After CNBr cleavage of hAT$_1$, the receptor fragments were lyophilised and resuspended in a buffer containing 25 mM Tris-HCl (pH 8.5), 1 mM EDTA, and 0.1% [w/v] SDS. The receptor fragments were dot-blotted onto a PVDF membrane by vacuum filtration. The membrane was then washed with water and air dried for 2 h. The following protocol is a modified version

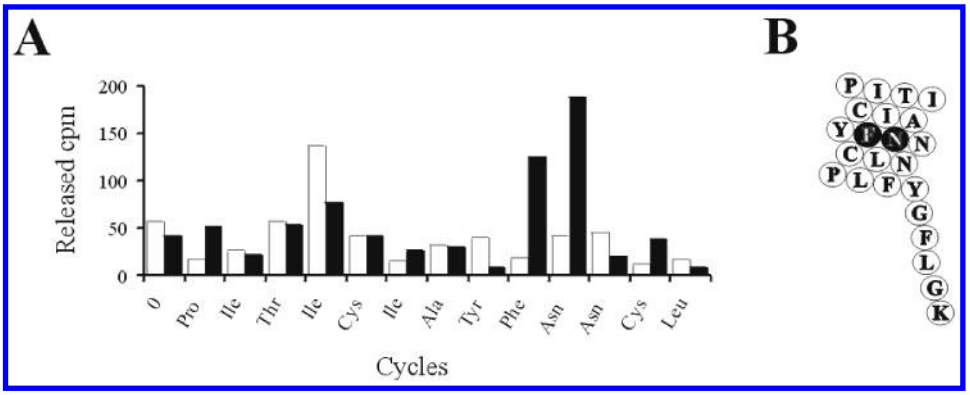

FIGURE 2: Edman degradation of the photolabeled CNBr fragment of the hAT_1 receptor. (A) The intact photolabeled and per-acetylated hAT_1 receptor (white columns) and its CNBr fragment (Pro^{285}-Met^{334}) (black column). (B) shows a schematic representation of contact sites of the AngII photolabel onto the hAT_1 receptor.

of that described by Ji et al (*14*). Briefly, the PVDF membrane containing the photolabeled receptor fragment (20000 to 2500 cpm) was washed with 1 mL of methanol followed by another washing with 1 mL of triethylamine. PITC-coupling for stepwise degradation was done by incubating the membrane for 30 min at 56 °C in 500 μL of triethylamine:methanol:PITC (1:7:1, [v/v]). The membrane was then washed with 1 mL of ethyl acetate, dried, and incubated for 5 min at 56 °C in 500 μL of TFA. Cleaved amino acids in form of phenylhydantoins were collected by washing with 1 mL of methanol and the radioactive content was evaluated by a γ-counter. Cycles were repeated as often as needed, starting by the washing step with triethylamine. Cycle 0 was done as described above, excluding the coupling step with PITC. To prevent concomitant degradation of the covalently linked peptide ligand during the repetitive cycles, proteins were acetylated with a 25-fold excess in concentration of sulfo-NHS acetate in a 100 mM borate buffer (pH 9) for 90 min prior to CNBr cleavage. Control experiments with nonacetylated, photolabeled receptor preparations were also carried out. Total radioactivity release during the cycles was generally in the range of >90% of the initial amount blotted onto the membrane. In a typical experiment (Figure 2), 2718 cpm were fixed on the PVDF membrane after washing and 2,327 cpm were released during the 16 cycles. A mean release rate of 58 cpm per cycle was observed during the noncleavage steps. Cycle efficiency was estimated from the radioactivity release at cycle 4 and 5 of the nonacetylated controls: unreacted amino functions would accumulate during the first 4 cycles, with the fourth being the release of the radiolabeled residue Tyr from the photolabeling peptide [Sar^1,Bpa^8]AngII. A radioactivity release at cycle 5 is thus an additive carry-over from the previous cycles. Mean cycle efficiency can therefore be estimated from this carry-over. In most experiments with nonacetylated receptor material, both unfragmented and CNBr-fragmented, this approach showed cycle efficiencies equal or above 98%. Experiments with lower efficiencies were rejected.

RESULTS AND DISCUSSION

In this study, we determined the contact sites between the C-terminal end of a photosensitive analogue of AngII and the hAT_1 receptor. [Sar^1,Bpa^8]AngII was previously characterized (*12*) as an antagonist with no inverse agonistic behavior (*31*, *32*). Therefore, it is important to keep in mind that the hAT_1 labeling occurs in its presumably inactive form.

Chemical cleavage of the photolabeled hAT_1 receptor with CNBr released a fragment of 7.2 kDa which corresponds to Pro^{285}∼Met^{334} as represented in Figure 1A and 5B. Since the interaction site of ^{125}I-[Sar^1,Bpa^8]AngII with the AT_1 receptor has been shown to occur within the first 11 amino acids (285−295) of the 7.2 kDa fragment (*12*), this CNBr fragment was now isolated and submitted to sequential Edman degradation.

Photolabeled hAT_1 receptor preparations were subjected to manual Edman degradation. On the fourth cycle, a significant radioactivity release was detected, both on intact receptors and on CNBr-fragmented preparations. This could indicate a labeling position on residue 4 of hAT_1 and/or degradation of the labeling peptide with release of the iodine labeled Tyr^4 residue. Ligand incorporation occurs however on the seventh transmembrane segment distal to residue 284 (*12*); therefore, all label release must be due to the release of the radiolabeled Tyr residue in the covalently attached labeling peptide. Consequently, the label attachment position on hAT_1 must be identical or distal to residue 288 in hAT_1. To minimize this confounding degradation of the labeling peptide, photolabeled receptor preparations were per-*N*-acetylated with sulfo-NHS-acetate in order to end-cap any free amino group, including the N-terminal amino function of the photolabeling peptide. Subsequent CNBr cleavage created then a new free N-terminus for the sequencing task. The structure−activity relationship of AngII on the AT_1 receptor unfortunately requires a primary or secondary amine in the N-terminal position. Acylated or alkylated (e.g., N−Acetyl or *N*,*N*-dimethyl) end-groups in AngII drastically reduce its affinity for AT_1 (*33*, *34*), thus protection of the N-terminal function must be introduced after binding and labeling. Figure 2A shows an example of radiosequencing of the per-acetylated hAT_1 receptor (open symbols). It revealed some radioactivity release at the fourth cycle due to incomplete acetyl protection of sarcosine on the incorporated photolabel followed by release of iodinated tyrosine at the fourth cycle. Identical treatment of photolabeled but nonacetylated hAT_1, both intact and after CNBr cleavage, produced a strong and practically total release of membrane-bound radioactivity at the fourth cycle (data not shown). Finally, radiosequencing of the labeled, per-acetylated, and CNBr-digested receptor showed a small radioactivity release, at step 4 on the 7.2 kDa fragment (Figure 2A, black bars), again probably due to incomplete acetyl protection. Important

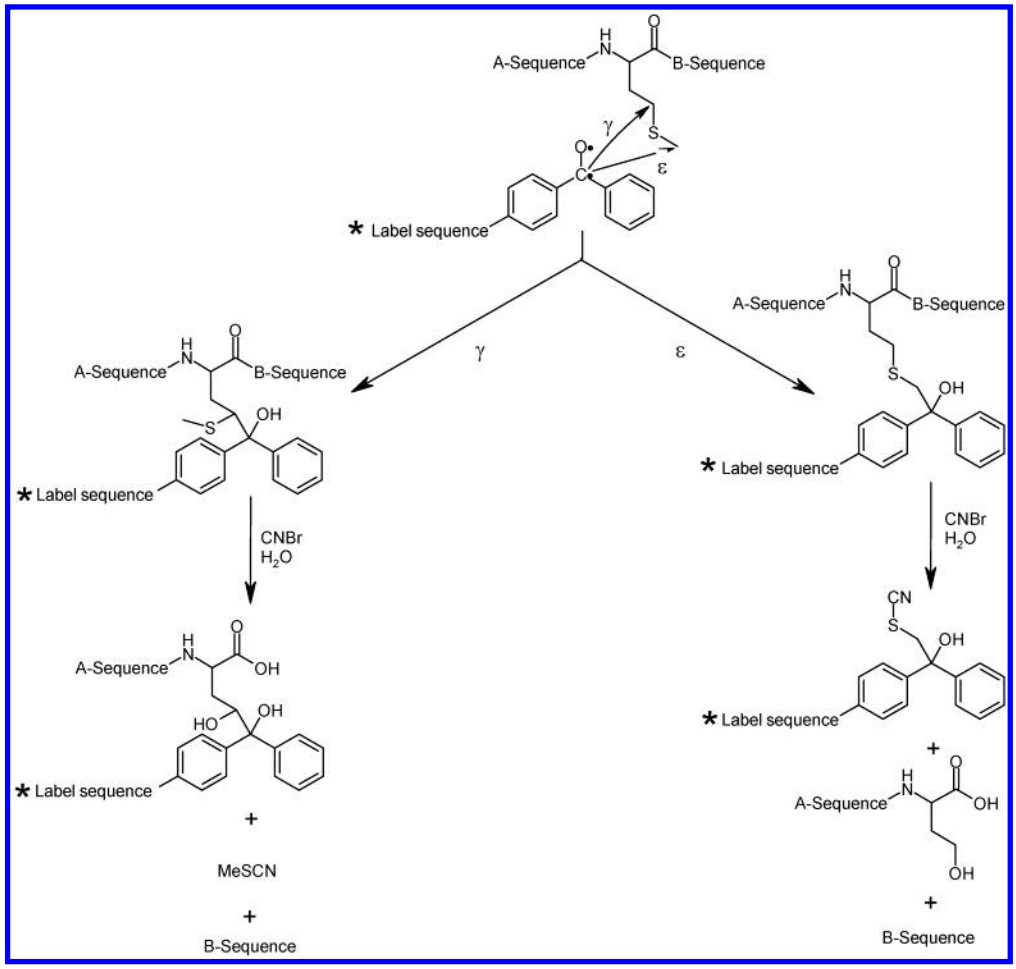

FIGURE 3: Reaction scheme of Bpa with Met residues and of CNBr cleavage. A sequence stands for the N-terminal receptor sequence and B-sequence for the C-terminal part. *Label sequence indicates the radioactively labeled (∗) photolabeling peptide residue on the benzophenone moiety.

radioactivity release is however observed at cycles 9 and 10, indicating an attachment of the photolabel at positions Phe^{293} and Asn^{294} (Figure 2B).

To confirm that Phe^{293} and Asn^{294} are indeed the contact sites for the C-terminal residue of the photosensitive AngII analogue, we created receptor mutants in which Phe^{293} or Asn^{294} were substituted for Met. The reasoning for this substitution was based on observations by Kage et al (*35*) who reported that a covalently linked photolabeling peptide, [Bpa^{8}]Substance P, was released from the NK-1 receptor following CNBr cleavage. They showed by mass spectrometry that the photolabeling peptide underwent an addition of an isothiocyanomethylene group to the benzophenone moiety, producing a tertiary alcohol. This addition was the result of the CNBr-induced cleavage of the thiomethyl ether of Met onto which the photolabel covalently linked itself during the photolabeling of the NK-1 receptor. This led to the determination of Met^{181} as the contact point in the amino acid sequence of the NK-1 receptor. The chemistry underlying the selective cleavage of CNBr on proteins is based on the thiolactone intermediate which is responsible for cleaving the peptide bond on the C-terminal side of Met residues followed by the release of the thiomethyl residue (Figure 3). In the event that the photolabel would be linked to the thiomethyl group at the end of the lateral chain of a Met residue, the intramolecular cleavage induced by CNBr would then release the photolabel modified by isothiocyanomethylation (*35*, *36*) (Figure 3, ϵ pathway). We reasoned that by mutating Phe^{293} and Asn^{294} for Met, the isothiocyanomethylated ^{125}I-[Sar^{1},Bpa^{8}]AngII would be released by cleavage with CNBr under the condition that ^{125}I-[Sar^{1},Bpa^{8}]-AngII is bound to the thiomethyl group.

In binding assays, both mutant receptors showed a high affinity for AngII. F293M-hAT_1 exhibited a Kd of 0.64 ± 0.03 nM whereas N294M-hAT_1 showed an affinity of 1.3 ± 0.4 nM, which are both similar to that of the wild-type hAT_1 receptor (0.5 ± 0.1 nM). The F293M-hAT_1 receptor also displayed good functionality as assessed by phospholipase C activation (Figure 4) after AngII stimulation. However, N294M-hAT_1 was essentially nonfunctional in the presence of AngII. Expression levels of both receptor mutants were similar to that of the wild-type receptor with Bmax values of 0.64 ± 0.22 pmol/mg for the wild-type, 0.63 ± 0.16 pmol/mg for F293M-hAT_1 and 0.37 ± 0.15 pmol/mg for N294M-hAT_1. The involvement of Asn^{294} into the activation mechanism of AT_1 has previously been recognized and attributed important trigger functions to this residue (*37*). The seventh TM has been early on recognized in several site-directed mutagenesis studies as being closely associated to ligand binding, especially of non-peptide ligands (*37*−*39*). Residue Asn^{294} has been associated to the AT_1 activation mechanism since the mutant N294A was essentially inactive in functional assays although peptide ligand binding was unaffected (*37*). Our observations on N294M support this

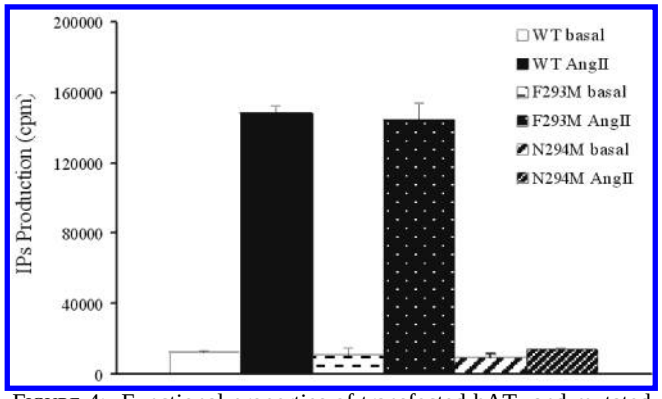

FIGURE 4: Functional properties of transfected hAT$_1$ and mutated hAT$_1$ receptors. COS-7 cells transiently expressing WT-hAT$_1$, F293M-hAT$_1$ or N294M-hAT$_1$ were labeled with *myo*-[^{3}H]inositol as described in the Experimental Section. Cells were incubated either in absence (basal) or in the presence of AngII 10^{-7}M for 20 min at 37 °C. Values represent the mean ±s.d. of triplicates from three independent experiments demonstrating identical results.

finding, showing an activation-impeded AT$_1$ mutant with normal AngII affinity. This Asn residue is highly conserved in the majority of GPCRs and its polar function is directly associated to receptor functionality. It is not surprising that the photolabeling amino acid is cross-linking to this area and this residue in particular since position 8 in AngII has always been closely associated to receptor activation and all potent peptide antagonists of AngII are position 8 analogues of AngII. The insertion into residue Phe^{293} should also be expected since the insertion reaction is supposed to be a function of proximity and van der Waals contact with more than one residue is to be expected in a densely packed environment. These aspects will be developed further below.

Figure 5A shows the CNBr cleavage of photolabeled mutants, F293M-hAT$_1$ and N294M-hAT$_1$. Cleavage generates a small fragment that migrated below the 3.4 kDa marker with the same electrophoretic mobility as ^{125}I-[Sar^1,Bpa^8]-AngII. This very low molecular weight fragment was not present in CNBr cleavage of the labeled wild-type hAT$_1$. Gel elution followed by HPLC in order to demonstrate an approximate resemblance between the photoproduct, a photolabel-isothiocyanate (1289 Da, Figure 3) and the original photolabel (1216 Da), was attempted but was not feasible due to the extremely low amounts available and due to the chemical nonidentity of the compounds to be compared (Figure 3). The presence of another fragment of larger size (apparent M_r = 4.2 kDa) is due to the expected labeling promiscuity to the labeling of the Met residue at a site beyond the thiomethyl group, e.g. on the Met γ carbon, according to the γ-pathway (Figure 3). In the case of F293M, we do not observe labeling of an additional possible protein fragment around 5.5 kDa (294−334) that could be attributed to concomitant labeling on the adjacent contact, Asn^{294}. However, this is not unexpected since, in our experience (*40*) and that of others (*41*), the thiomethyl moiety of Met placed in immediate proximity of the labeling residue has a tendency to monopolize the labeling process. Therefore, in the case of F293M photolabeling, the attachment is expected to occur exclusively on the 293rd residue. Altogether, these results suggest that the modified photolabel is released only if cross-linked to the thiomethyl group of Met residues.

Two further mutants were created with their Met residues inserted on the N-terminal side and on the C-terminal side

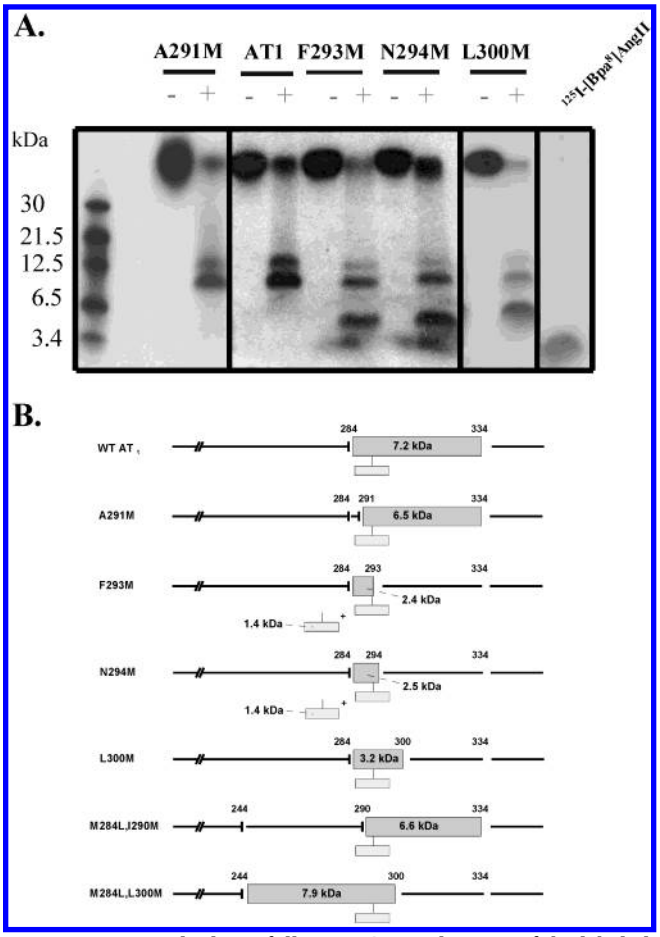

FIGURE 5: Ligand release following CNBr cleavage of the labeled hAT$_1$ receptor and its labeled mutants. (A) Photolabeled A291M-hAT$_1$, WT-hAT$_1$, F293M-hAT$_1$, N294M-hAT$_1$, and L300M-hAT$_1$ were submitted to CNBr cleavage (100 mg/mL). The digestion products were submitted to SDS−PAGE. ^{14}C-labeled protein standards of the indicated molecular masses (kDa) and the free photolabel were run in parallel. Three independent experiments demonstrated identical results. (B) Schematic representation of the expected CNBr cleavage fragments from photolabeled hAT$_1$ receptor and its Met-mutants. Theoretical molecular weights are indicated in kDa of the presumably radioactive fragments (shaded boxes). The photoligand is indicated as a small rectangle and the Met cleavage positions are indicated above.

of the attachment position: A291M-hAT$_1$ and L300M-hAT$_1$. These two mutants were not distinguishable from hAT$_1$ in expression level (0.70 pmol/mg and 0.63 pmol/mg), Ang II binding (2.70 nM and 0.80 nM) and inositol production (data not shown). As expected, photolabeling of mutant L300MhAT$_1$ with subsequent CNBr cleavage (Figure 5A, right panel) produced a low molecular weight fragment (apparent M_r 5.0 kDa) similar to those of the two contact point mutants F293M- and N294M-hAT$_1$. It also appears to be of some reduced electrophoretic mobility due to its larger molecular weight (2371 Da for N294M vs 3025 Da for L300M, Figure 5B). Most importantly, the mutant L300M did not produce the lowest molecular weight band presumably the released photolabel migrating similar to the free ligand. This experiment confirms (A) that ligand release happens only if Met is in the immediate vicinity of the contact and labeling occurs therefore on the thiomethyl moiety and (B) that the very low molecular weight fragment is indeed the released, modified form of the ligand. After photolabeling and CNBr digestion, the mutant A291MhAT$_1$ produced a pattern identical to that

of WT hAT_1 (Figure 5A, left parts, and 5B) with only a larger molecular weight protein fragment with photolabel attached to it (292−334 instead of 295−334). Complete absence of ligand release indicates labeling not on 291 but at later residues, i.e., 293/294. Our results are consistent with those obtained in a previous study in which we showed that ^{125}I-[Sar^1,Bpa^8]AngII seemed to label the oligopeptide 285−295 within the seventh transmembrane domain of the hAT_1 receptor (*12*). The small differences in the observed electrophoretic mobility in fragments with apparent molecular weight below 5 kDa and the relative variability of migration in SDS−PAGE of small hydrophobic peptides with strong helical character do not allow the unambiguous assignment of exact molecular weights to the observed fragments. The appearance of released photolabel through the CNBr reaction cannot be distinguished from the small protein fragments through molecular weight determination but rather by their relative electrophoretic mobility, their rapid diffusion comparable to that of the photoligand and, most importantly, by their absence in the two mutants A291M and L300M-hAT_1. To confirm the nature of the small protein fragments observed, two further AT_1 mutants were constructed with the Met^{284} replaced by Leu. This would permit the creation of much larger fragments from the Met-mutants in the contact area upon CNBr cleavage and to distinguish further from eventually released octapeptide ligand through the CNBr reaction (Figure 5B). The following two mutants were added to the study: M284L,I290M-hAT_1 and M284L,L300M-hAT_1. Both mutants displayed expression levels (Bmax 0.37 (M284L, I290M) and Bmax 0.55 (M284L, L300M) pmol/mg) and AngII binding properties (Kd's of 0.61 nM for M284L,I290M-hAT_1 and of 0.57 nM for M284L,L300M-hAT_1) comparable to those of hAT_1. Photolabeling of both mutants produced intense photolabeling with yields comparable to that of WT-hAT_1. However, upon CNBr cleavage, the M284L,L290M-hAT_1 mutant produced a strong protein band around 6.3 kDa with no trace of ligand release (not shown). The observed protein fragment must correspond to the expected 291−334 fragment, indicating a label position distal to 290. Mutant M284L,L300M-hAT_1 produced, upon photolabeling and subsequent CNBr cleavage, a fragment of 7.0 kDa, corresponding to the sequence 245−300. As for the previous mutant, no trace of ligand release was observed (not shown). These two mutants further confirm the assignment of positions 293 and 294 as the immediate contact points of the C-terminal amino acid of the photoactive ligand as well as the nature of the observed small protein fragments. Studies are currently underway with agonistic photolabels and constitutively active receptor mutants to evidence and understand eventual changes in ligand−receptor interactions following receptor activation.

Previous results showed a ligand−receptor contact to occur between residues Pro^{285} and Asn^{295} (*12*, *20*). The Edman degradation experiments presented herein are strongly suggestive of residues Phe^{293} and Asn^{294} as contact points. The contact mutants F293M and N294M produce ligand release upon photolabeling and successive CNBr cleavage, thus confirming contact with 293 and 294. Finally, the last mutants indicate contact beyond 291 yet before 300.

So far, the evidence gathered indicates that labeling occurs between position 291 and 295 on residues 293 and 294 of the hAT_1 receptor. Comparing this area of the hAT_1 receptor

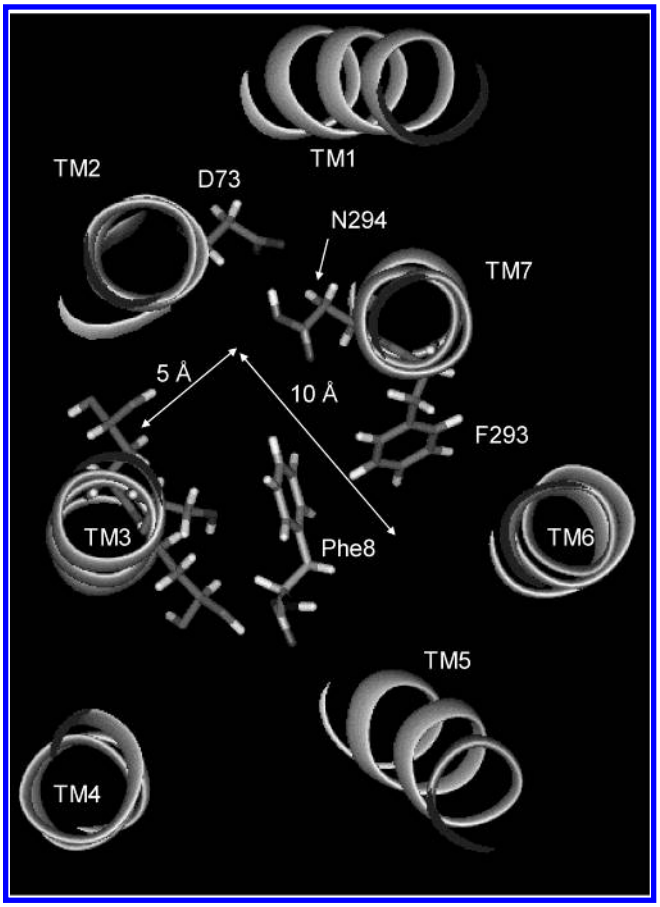

FIGURE 6: Molecular modeling of ligand occupied hAT_1. The present view is a horizontal section (viewed from extracellular space) of 25 −35 Å from the cell surface of the previously proposed model (*20*). The contact residues Phe^{293} and Asn^{294} are identified as well as the residues of TM3 facing the crevice that accommodates the aromatic ring of position 8 of AngII. The depicted residues of TM3 are (from top) Leu^{118}, Ser^{115}, and Leu^{119}.

with several other typical GPCRs is not straightforward since no exact topographical information is available yet, with the exception of bovine rhodopsin. According to the consensus of TM structure alignments with respect to the most conserved residues and motifs, as proposed by Ballesteros and Weinstein (*42*), residues Phe^{293} and Asn^{294} should be numbered 7.44 and 7.45, calculated from their position and the closely following NPXXY-motif. Asn^{295} has been the target of many hypotheses of receptor activation where hydrogen bonding to other polar receptor function were proposed, e.g., Asn^{111} and Asp^{74} (*43*). Examining more closely the receptor structure proposed in our earlier contribution (*20*), in the area of interest (i.e., the interaction area where the phenylalanine residue 8 of AngII is lodged) we can now make several observations: Residue Phe^{293} (one of the contact points) is at the same location as Lys^{297} in bovine rhodopsin, the attachment point of the retinal chromophore and pointing into the center of the receptor body. Asn^{294} (the other contact residue) appears to be positioned opposite to TM2 and forming a 1.66 Å hydrogen bridge with Asp^{74}. The geometry of the TM elements 3, 2, and 7 forms at this level, 25 Å below the presumed interface of the membrane and of the extracellular space, a roughly rectangular space of 5 Å by 10 Å (Figure 6). Phe^{293} and Asn^{294} point toward the space where the aromatic residue of Phe^8 of Ang II is located. This 5 Å × 10 Å space also accommodates the benzophenone

moiety of [Sar[1],Bpa[8]]AngII that led to the present study. The modeling and energy minimization was carried out in the presence of the natural Phe[8] residue in AngII (*20*) and not Bpa[8]. Considering earlier accumulated structure−activity relationship information on position 8 modified AngII analogues, highly compatible considerations corroborating the above views become possible: In the series of position 8 aromatic analogue of AngII, a gradual transition from agonistic toward partial agonistic and finally purely neutral antagonistic properties was observed. The affinity of all those analogues remained in general unaffected, i.e., in the low nM range, reflecting an unchanged free energy from the binding process. [Sar[1],Bpa[8]]AngII, [Sar[1],*p*-N_3Phe[8]]AngII (*44*), [Sar[1],*p*-BrPhe[8]]AngII (*45*), and similar analogues are all full agonists. Increasing the number of substituents and their size showed however a trend toward reduced intrinsic activity, e.g., [Sar[1],*p*-I−Phe[8]]AngII (*45*) retained 80% intrinsic activity and the multi substituted [Sar[1],*m*,*m*-Br_2-*p*-Cl−Phe[8]]AngII (*45*) was already reduced below 50%. The fully substituted [Sar[1],Br_5Phe[8]]AngII (*45*) was however a complete antagonist as well as [Sar_1,Pyr[8]]AngII (where Pyr stands for the polynuclear aromatic 4-L-pyrenylalanine) and the present [Sar[1],Bpa[8]]AngII. The aromatic residues of position 8 of antagonistic peptides, e.g. [Sar[1],Bpa[8]]AngII do practically fill out this space, whereas agonists, e.g. Phe[8], leave several Å free apical space toward TM2, giving some freedom of movement to Asn[294] for a conformational change associated to receptor activation. Further corroborating information may be gathered from other more exotic aromatic position 8 AngII analogues: If Phe[8] is replaced by residues that show a much more important van der Waals diameter perpendicular to the aromatic π plane then important affinity effects were observed, presumably by disturbing the binding pocket beyond its 5 Å width. [Sar[1],L-*o*-Carboranylalanine[8]]-AngII (*46*) has a spherical aromatic side chain with a residue diameter of 7.66 Å and a concomitant 800-fold affinity loss compared to [Sar[1]]AngII. The bulky but high affinity peptide antagonists, e.g. [Sar[1],Pyr[8]]AngII and [Sar[1],Bpa[8]]AngII, have a π-perpendicular diameter below 4 Å, which is similar to that of Phe. They would not disturb the 5 Å × 10 Å pocket but should fully occupy it.

In conclusion, our view of an extended peptide ligand is supported by contact of residue 3 of AngII with residue 172 of hAT_1 and contact of residue 8 of AngII with position 293 and 294 of hAT_1. This implies that AngII must interact in an extended form, more or less parallel to the transmembrane domains of the hAT_1 receptor. Our recent results on hAT_2 show for AngII a similar ligand organization (*47*), opening up the speculation that such a receptor−ligand interaction could be found also in other peptidergic systems.

ACKNOWLEDGMENT

We thank Mrs. M.-R. Lefebvre for her expert help and technical assistance and Mrs. M.-C. Hopper for her help in producing this manuscript.

REFERENCES

1. Peach, M. J. (1981) *Biochem. Pharmacol. 30*, 2745−51.
2. Hein, L., Barsh, G. S., Pratt, R. E., Dzau, V. J., and Kobilka, B. K. (1995) *Nature 377*, 744−7.
3. Ichiki, T., Labosky, P. A., Shiota, C., Okuyama, S., Imagawa, Y., Fogo, A., Niimura, F., Ichikawa, I., Hogan, B. L., and Inagami, T. (1995) *Nature 377*, 748−50.
4. Horiuchi, M., Akishita, M., and Dzau, V. J. (1998) *Endocr. Res. 24*, 307−14.
5. Sasaki, K., Yamano, Y., Bardhan, S., Iwai, N., Murray, J. J., Hasegawa, M., Matsuda, Y., and Inagami, T. (1991) *Nature 351*, 230−3.
6. Murphy, T. J., Alexander, R. W., Griendling, K. K., Runge, M. S., and Bernstein, K. E. (1991) *Nature 351*, 233−6.
7. Kambayashi, Y., Bardhan, S., Takahashi, K., Tsuzuki, S., Inui, H., Hamakubo, T., and Inagami, T. (1993) *J. Biol. Chem. 268*, 24543−6.
8. Servant, G., Laporte, S. A., Leduc, R., Escher, E., and Guillemette, G. (1997) *J. Biol. Chem. 272*, 8653−9.
9. Hjorth, S. A., Schambye, H. T., Greenlee, W. J., and Schwartz, T. W. (1994) *J. Biol. Chem. 269*, 30953−9.
10. Inoue, Y., Nakamura, N., and Inagami, T. (1997) *J. Hypertens. 15*, 703−14.
11. Paiva, A. C. M., Costa-Neto, C. M., and Oliveira, L. (1998) in *Proceedings of INABIS '98 Conference: Fifth Internet World Congress on Biomedical Sciences at McMaster University*, http://www.mcmaster.ca/inabis98/escher/paiva0625.
12. Laporte, S. A., Boucard, A. A., Servant, G., Guillemette, G., Leduc, R., and Escher, E. (1999) *Mol. Endocrinol. 13*, 578−86.
13. Mukoyama, M., Nakajima, M., Horiuchi, M., Sasamura, H., Pratt, R. E., and Dzau, V. J. (1993) *J. Biol. Chem. 268*, 24539−42.
14. Ji, Z., Hadac, E. M., Henne, R. M., Patel, S. A., Lybrand, T. P., and Miller, L. J. (1997) *J. Biol. Chem. 272*, 24393−401.
15. Phalipou, S., Cotte, N., Carnazzi, E., Seyer, R., Mahe, E., Jard, S., Barberis, C., and Mouillac, B. (1997) *J. Biol. Chem. 272*, 26536−44.
16. Corbin, J., Wang, H. H., and Blanton, M. P. (1998) *Biochim. Biophys. Acta 1414*, 65−74.
17. Li, Y. M., Marnerakis, M., Stimson, E. R., and Maggio, J. E. (1995) *J. Biol. Chem. 270*, 1213−20.
18. Dong, M., Wang, Y., Hadac, E. M., Pinon, D. I., Holicky, E., and Miller, L. J. (1999) *J. Biol. Chem. 274*, 19161−7.
19. Nikiforovich, G. V., and Marshall, G. R. (2001) *Biochem. Biophys. Res. Commun. 286*, 1204−11.
20. Boucard, A. A., Wilkes, B. C., Laporte, S. A., Escher, E., Guillemette, G., and Leduc, R. (2000) *Biochemistry 39*, 9662−70.
21. Sakarellos, C., Lintner, K., Piriou, F., and Fermandjian, S. (1983) *Biopolymers 22*, 663−87.
22. Joseph, M. P., Maigret, B., and Scheraga, H. A. (1995) *Int. J. Pept. Protein Res. 46*, 514−26.
23. Johannesson, P., Lindeberg, G., Johansson, A., Nikiforovich, G. V., Gogoll, A., Synnergren, B., Le Greves, M., Nyberg, F., Karlen, A., and Hallberg, A. (2002) *J. Med. Chem. 45*, 1767−77.
24. Bosse, R., Servant, G., Zhou, L. M., Boulay, G., Guillemette, G., and Escher, E. (1993) *Regul. Pept. 44*, 215−23.
25. Fraker, P. J., and Speck, J. C., Jr. (1978) *Biochem. Biophys. Res. Commun. 80*, 849−57.
26. Laporte, S. A., Servant, G., Richard, D. E., Escher, E., Guillemette, G., and Leduc, R. (1996) *Mol. Pharmacol. 49*, 89−95.
27. Nakamaye, K. L., and Eckstein, F. (1986) *Nucleic Acids Res. 14*, 9679−98.
28. Downes, C. P., Hawkins, P. T., and Irvine, R. F. (1986) *Biochem. J. 238*, 501−6.
29. Laemmli, U. K. (1970) *Nature 227*, 680−5.
30. Blanton, M. P., and Cohen, J. B. (1994) *Biochemistry 33*, 2859−72.
31. Groblewski, T., Maigret, B., Larguier, R., Lombard, C., Bonnafous, J. C., and Marie, J. (1997) *J. Biol. Chem. 272*, 1822−6.
32. Pérodin, J. (2000) Ph.D Thesis, Université de Sherbrooke, Sherbrooke.
33. Bouley, R., Perodin, J., Plante, H., Rihakova, L., Bernier, S. G., Maletinska, L., Guillemette, G., and Escher, E. (1998) *Eur. J. Pharmacol. 343*, 323−31.
34. Regoli, D., Rioux, F., Park, W. K., and Choi, C. (1974) *Can. J. Physiol. Pharmacol. 52*, 39−49.
35. Kage, R., Leeman, S. E., Krause, J. E., Costello, C. E., and Boyd, N. D. (1996) *J. Biol. Chem. 271*, 25797−800.
36. Bisello, A., Adams, A. E., Mierke, D. F., Pellegrini, M., Rosenblatt, M., Suva, L. J., and Chorev, M. (1998) *J. Biol. Chem. 273*, 22498−505.
37. Hunyady, L., Ji, H., Jagadeesh, G., Zhang, M., Gaborik, Z., Mihalik, B., and Catt, K. J. (1998) *Mol. Pharmacol. 54*, 427−34.
38. Karnik, S. S., Husain, A., and Graham, R. M. (1996) *Clin. Exp. Pharmacol. Physiol. Suppl. 3*, S58−66.

39. Perlman, S., Schambye, H. T., Rivero, R. A., Greenlee, W. J., Hjorth, S. A., and Schwartz, T. W. (1995) *J. Biol. Chem. 270*, 1493−6.
40. Rihakova, L., Deraët, M., Auger-Messier, M., Pérodin, J., Boucard, A. A., Guillemette, G., Leduc, R., and Escher, E. (2002) *J. Rec. Sig. Trans. Res.* (in press).
41. Macdonald, D., Mierke, D. F., Li, H., Pellegrini, M., Sachais, B., Krause, J. E., Leeman, S. E., and Boyd, N. D. (2001) *Biochemistry 40*, 2530−9.
42. Ballesteros, J. A., and Weinstein, H. (1995) in *Methods in Neurosciences* (Sealfon, S. C., and Fishberg, D. A. M., Eds.) pp 366−428, Academic Press, New York.
43. Balmforth, A. J., Lee, A. J., Warburton, P., Donnelly, D., and Ball, S. G. (1997) *J. Biol. Chem. 272*, 4245−51.
44. Escher, E. H., Nguyen, T. M., Robert, H., St-Pierre, S. A., and Regoli, D. C. (1978) *J. Med. Chem. 21*, 860−4.
45. Leduc, R., Bernier, M., and Escher, E. (1983) *Helv. Chim. Acta 66*, 960−70.
46. Escher, E., Guillemette, G., Leukart, O., and Regoli, D. (1980) *Eur. J. Pharmacol. 66*, 267−72.
47. Deraet, M., Rihakova, L., Boucard, A., Perodin, J., Sauve, S., Mathieu, A. P., Guillemette, G., Leduc, R., Lavigne, P., and Escher, E. (2002) *Can. J. Physiol. Pharmacol. 80*, 418−25.

BI0258602